Some Guidelines on CT-Scanning for Fluid Flow Visualization and Quantification

Shameem Siddiqui[1,2*]

[1]Halliburton Consulting, 3000 N. Sam Houston Pkwy, E, Houston, TX 770, USA
[2]ResVisions LLC, 16902 Cook Landing Drive, Richmond, TX 77407

Abstract. One of the first uses of CT-scanning in the oil and gas industry has been for visualizing multiphase fluid flow in porous media. The density and effective number contrast between fluids flowing in porous media forms the basis of fluid visualization using CT. Accurate measurement of fluid saturation requires proper selection of type and concentration of radiopaque tracers and the preparation of core samples. In this paper some useful guidelines are provided for obtaining meaningful quantitative results from CT-based multiphase flow experiments. Compared to whole core CT-scanning for petrophysical applications, CT-based flow visualization requires elaborate laboratory setup, with special equipment and materials, to ensure its success. This paper makes some practical suggestions for setting up the lab equipment for multiphase flow visualization with CT. Although saturation data on fluids inside the core can also be obtained from linear X-ray devices, CT provides both qualitative and quantitative information such as gravity and capillary effects, viscous fingering and heterogeneity effects in 3D, which provides lot of insights into a SCAL experiment. This paper gives some insights into the selection of radiopaque tracers for typical two-phase flow experiments. It also includes discussion on how to match two dopants to have the same response so that they can be treated as one fluid, which is useful when only a single energy scan can be used. The paper also discusses CT image subtraction, which separates the matrix from the fluid and thus enhances the ability to view the interaction between individual fluids, with some examples from actual experiments. CT has been successfully used in many SCAL experiments to answer some very critical questions regarding rock and fluid heterogeneity. In addition, CT has been used for measuring pore volume compressibility, observing wormhole development during acid injection and quantifying fluid heterogeneity. This paper demonstrates several successful applications of CT-scanning in multiphase flow, rock property measurement and treatment of rock with different treating chemicals. Guidelines provided in this paper can help broaden our understanding of reservoirs

1 Introduction

CT-scanners have been used since the 1970s for scanning mainly human subjects. From the very beginning, the non-destructive and non-invasive aspects of CT-scanning showed enormous potential to enhance the quality of research in several other engineering fields. One of the disciplines benefiting from the use of CT for research is the oil and gas sector, for which CT was able to provide valuable qualitative and quantitative information on multiphase flow through porous media. Wang et al. [1] described one of the earliest uses of CT-scanning for obtaining images of water and oil saturations during coreflooding in Berea sandstone cores. Cromwell et al. [2] performed some two-phase displacement tests and were able to locate the Buckley-Leverett shock front inside the core during the displacement of mineral oil by a tagged brine solution. Vinegar and Wellington [3], Wellington and Vinegar [4], and Withjack [5] were among the first to provide comprehensive methodologies for the application of CT-scanning for coreflooding as well as for core characterization. Comprehensive reviews of CT applications for fluid flow visualization and quantification can be found in the literature [3-10].

The following list includes some of the areas in which CT has been able to contribute in the broad category of fluid flow visualization and quantification.

- Measuring saturations in coreflooding experiments for relative permeability,
- Measuring pore volume compressibility
- Evaluating fractures and flow in fractures
- Visualization of foam flow in porous media and application in foam diversion in acidizing.
- Study of viscous instabilities and gravity segregation in multiphase flow through porous media.
- Design of improved enhanced oil recovery techniques, effect of the injection of different chemicals
- Acid treatment of formation rocks and selection of proper additives.
- Observation of wormhole development and growth during acidizing
- Evaluation of set cement and concrete

Unlike CT-scanning for whole core analysis, CT-based flow visualization and quantification requires an elaborate laboratory setup with a capability to mimic reservoir conditions, if necessary. In order to increase the contrast between the different fluid phases, one or more of the fluids

* Corresponding author: siddiqui.shameem@gmail.com

are tagged (or doped) with radiopaque tracers. In the following sections we will deal with these different items individually.

2 CT-Scanner

As far as choice of CT-scanner, one can use either the medical or industrial type CT-scanners, each of which has its own advantage and disadvantage. In a medical CT scanner, the subject (coreholder) does not rotate but goes back and forth inside the CT gantry. This is ideal for coreflooding applications. The overall fast scanning speed allows the scanner to outrun the flow rate of the fluids. When it comes to working with cores in a vertical configuration, it is a bit more challenging, as the medical scanner gantry needs to be put in a horizontal position and there should be a positioning system for handling the core holder vertically. This has been successfully done at the research facilities of three US universities (University of Houston, Stanford University and University of Wyoming). Another disadvantage of medical scanners is that most have the pixel resolution of about 0.5 mm x 0.5 mm, which is much larger than a typical pore size, and it is not possible to resolve small-scale heterogeneities. With the multi-slice technology however, there has been significant improvement in axial resolution. At a macro scale, the medical scanners perform satisfactorily for visualizing and quantifying two- and three-phase saturations.

Industrial CT-scanners, of which the micro CT-scanners are a subset, generally provide a much better pixel resolution (smaller than 0.2 mm x 0.2 mm) than the medical scanners, and they are ideally suited for the core in a vertical configuration. They are also not limited by the 150 kV operating voltage of the medical CT-scanners, which can sometimes limit the use of the latter when scanning high-density materials, larger diameter cores or using a coreholder made from thicker or denser materials.

However, most industrial (and micro) CT-scanners require the subject to be rotated during the scanning, which can create several issues as far as flow visualization. Since the scanning speed is relatively slow and the sample is generally rotating back and forth, some artifacts in flow measurement can be expected. The fact that the coreholder needs to be rotated means that part of the fluid lines to and from the coreholder will need to be rotated too, requiring quite an elaborate setup for the flow system to work correctly. Recent advances in micro-CT scanners, such as the Tescan DynaTom®, with about 10 μm x 10 μm resolution and with the source and detector rotating around the static coreholder, is a clear breakthrough. With this, it is now possible to use dynamic imaging at a very high spatial resolution at a relatively high speed.

3 Coreflooding Equipment

The reservoir condition tests involve mimicking the reservoir pressure and temperature reasonably accurately. This requires a reservoir condition coreflooding setup as well as special coreholders and fluid lines.

Unlike regular coreflooding setup, in which the coreholder and fluid cylinders are kept inside a large oven, the CT coreflooding system must have the components split into two areas. The fluid cylinders and floating piston accumulators, pump hydraulic parts and acoustic separators can still be kept inside an oven but the coreholder and some flow lines have to be mounted inside the CT gantry with adequate insulation and flexible connections.

For CT flow experiments a low X-ray attenuation coreholder is necessary as the standard stainless steel or Hastelloy coreholders have a tendency to scatter the X-ray beams. Low X-ray attenuation coreholders (see Fig. 1) manufactured with an Aluminum alloy sleeve wrapped with a graphite fiber composite outer body (such as the Temco/CoreLab Instruments FCH® series coreholders) have been widely used for CT flow experiments at pressures as high as 10,000 psi and temperatures as high as 300° F. Coreholders made from Titanium, Aluminum alloy, Beryllium and Acrylic have also been used by various researchers for different pressure and temperature conditions.

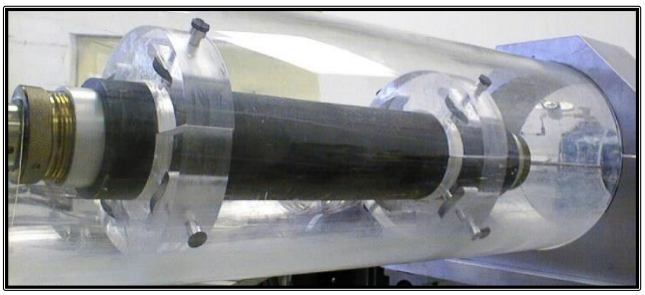

Fig. 1. Photograph of a low X-ray attenuation coreholder securely positioned inside a Plexiglas tube for CT-scanning with fluid flow.

As for the temperature control, since the coreholder cannot be put inside an oven, reservoir temperature inside the coreholder level can be attained by one of at least three methods. The first is to use heating tapes with temperature controllers, assuring that no metallic coils are within the scanning area. The second is to use heated stainless steel end plugs with temperature controllers. The third and the most effective method is to use a recirculation heating system that circulates a hot fluid (such as ethylene glycol, furnace oil, etc.) into the annular space between the Hassler sleeve and the inner wall of the coreholder. The heating fluid should be compatible with the sleeve material and also should not affect the X-ray attenuation significantly. It should be noted that the coreholder pre-hardens the X-rays and therefore the beam hardening effect is less significant in a typical CT flow experiment. In order to maintain a uniform temperature throughout the experiment, the coreholder and all the flowlines should be insulated with X-ray transparent insulators and temperature should be monitored continuously with temperature sensors. Fig. 2 shows a recirculating heating system along with backpressure and confining pressure regulators.

Fig. 2. Photograph of a recirculating heating system (right) with backpressure regulator and confining pressure regulator (left).

As for the flow lines, the standard stainless-steel tubing (with insulation, as necessary) can be used throughout the system, except for the scanning area. Presence of stainless-steel tubing in the scanning area causes X-rays to scatter and cause problems during image processing. It should be noted that only the coreholder bypass lines (one for each phase) and the pressure tapping lines for differential pressure are the ones that can potentially be in the scanning area. PEEK (polyether ether ketone) tubing (3000 psi burst rating for 1/8" OD) can be used in place of stainless steel for the bypass lines because the pressure does not have to be very high in those lines. The two pressure taps (upstream and downstream) on the cores used for differential pressure measurement with diaphragm type transducers can be replaced by two absolute pressure transducers mounted at the inlet and outlet of coreholder, respectively.

Since a research CT-scanner can have multiple uses, rather than having a permanent setup around the CT-scanner, it may be a good idea to build a portable coreflooding unit that can be moved around to accommodate other types of activities, such as whole core scanning or plug characterization for sample selection. Fig. 3 shows the schematic of a portable coreflooding unit designed to be used for CT flow visualization and quantification experiments [11]. Fig. 4 shows the photograph of such a system during an actual CT-assisted flow experiment [12].

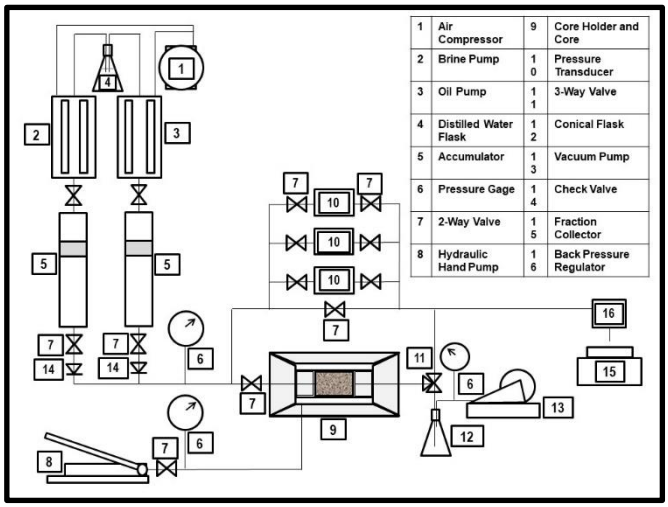

Fig. 3. Schematic of portable coreflooding unit designed to be used for CT flow visualization experiments [11].

Fig. 4. Photograph of a CT-scanner using a portable coreflooding unit for a flow visualization study [12].

4 Dopants

Fluid flow visualization with CT almost always involves the use of one or more radiopaque tracers (also called dopants or tagging agents). The mass attenuation coefficient (or the normalized CT number), which is measured by a CT-scanner is a function of both density and effective atomic number. In a typical multiphase flow setting, there is not enough density contrast between the different fluid phases and therefore the contrast is provided by the high effective atomic number of the dopant. Vinegar and Wellington [3] conducted detailed research on the dopants for using in the oil, brine and gas phases. Some of the dopants mentioned by them are, Sodium Iodide, Sodium Bromide, Sodium Molybdate, Sodium Tungstate, etc. (water-soluble); iodo-dodecane, iodo-hexadecane, etc. (oil-soluble); and Xenon and Krypton (gas soluble). It should be noted that the price of dopant can sometimes be a factor in dopant selection, especially since very high purity dopant is required to avoid uncertainties in saturation measurements. Use of one dopant is sufficient for a two-phase flow experiment and two are sufficient for a three-phase flow experiment. Sahni et al. [13] successfully used two X-ray energies to calculate saturations during three phase flow experiments. Sodium iodide (NaI) has relatively high solubility in water (2278 g/l at 122 °F) and it is one of the most common dopants used in CT flow studies. Usually, all reservoir brines contain sodium chloride (NaCl), so replacing some of the Cl- ions with I- ions does not make the brine too different. Some researchers [14] have reported using potassium iodide (KI) for clay-rich core samples.

The appropriate concentration of dopant to be used can be found using a trial-and-error process. In general, the dopant concentration should be increased for low-porosity cores in order to get sufficient contrast between the different phases. Once a dopant with a sufficient contrast has been selected for a study (say 5% by weight of NaI in the brine phase), a sample of the doped brine should be preserved in a plastic (e.g., HDPE) or glass bottle (with no air bubble) of preferably the same diameter as the core, for calibration purposes. This bottle should then be scanned inside the coreholder, inside the Hassler sleeve, at the same X-ray energy at which the coreflooding test would be performed, for calibration purposes. Similarly, an (air-filled) empty bottle of the same size should also be scanned under the same condition, for

calibration. In the early days of fluid flow visualization research with CT-scanners, calibration rods (small 1 cm diameter tubes filled with dopant, air, etc.) were mounted (taped) outside the coreholder but the data were prone to errors because of very small region of interest inside these tubes and also due to different attenuation conditions (inside versus outside the coreholder). Scanning these calibration samples inside the coreholder always provides better results.

5 Core Preparation

For multiphase flow visualization and quantification, the core plugs should ideally be cleaned, extracted (in a Soxhlet extractor, with one, and sometimes more than one solvent) and dried before the actual test. It is also recommended to conduct helium porosimetry measurements on all the plugs for comparing with CT based measurements. For tests with composite core plugs (for better representation of the heterogeneity within a section of reservoir) it is strongly recommended to mill the two ends of each core plug for a perfect fit with the adjacent plug and to ensure good capillary continuity. Gaps between core plugs due to plug cutting errors will have a tendency to retain fluids, using filter paper between two plugs for ensuring capillary continuity will also result in undesirable fluid retention, potentially causing some anomalies in saturation calculation. Fig 5. Shows an example of the effect of fluid retention at the interface between two core plugs in a three-plug composite core during a steady-state supercritical CO2-brine relative permeability test [14].

In order to maintain the confining pressure on the core plugs, they are placed inside the Hassler sleeve before being mounted inside the coreholder. Coating with epoxy or wrapping with Teflon tape can sometimes be used to mitigate surface anomalies. For a CT setup, the confining pressure is applied using either a hand pump or the recirculating heating system, depending on the requirement of the test. For experiments at higher than ambient temperature, all the flow lines, accumulators and coreholder parts should be properly insulated and the temperatures should be closely monitored to maintain the desired temperature.

It is strongly recommended to securely fasten the coreholder in the positioning table with retaining screws, tapes, or other fastening devices so that it cannot move freely during the scanning. Minor movement of the coreholder can potentially create undesirable image artifacts. The CT scanner's table positioning system should also have very good positional accuracy to be able to start scanning from the exact same location each time in order to ensure proper data analysis through image subtraction.

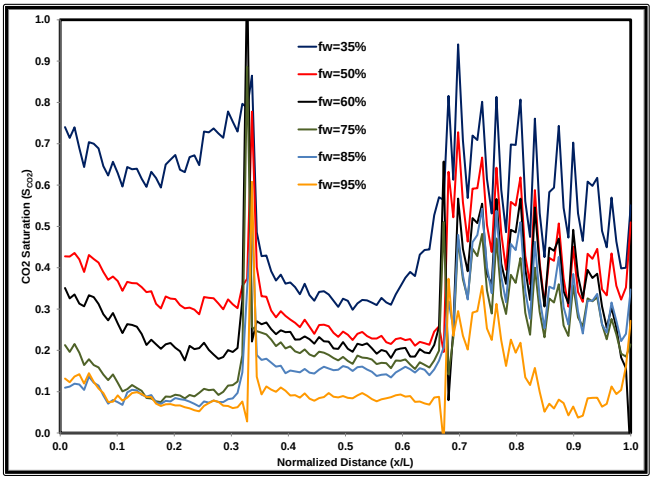

Fig. 5. CT-derived saturation distribution in the St. Peter composite core using steady-state technique showing anomalous saturation values at the interface between two adjacent core plugs in a three-plug composite core [15].

6 Porosity Measurement

The only quantitative data that a CT-scan slice provides is the Mass attenuation coefficient, which comes from the Beer's law and is a function of both effective atomic number and density. For the industrial and micro CT-scanners, the mass attenuation coefficient is typically simplified to an 8- or 12-bit grayscale number. For the medical CT-scanners the attenuation is expressed in CT number (CTN, in Hounsfield units) for which the medical CT scanners are calibrated to read a value of -1000 for air and 0 for water. In this paper we will use CTN and grayscale numbers interchangeably.

Porosity measurement is one of the first tests conducted in a CT flow visualization test. The method is analogous to the vacuum saturation method for measuring porosity but instead of weighing the sample before and after saturation, the average CTN at each location is used, along with the average CTN for the two calibration samples discussed above (air and doped water).

Porosity is measured by scanning the core at several locations when it is dry and then scanning the core at the same precise locations after it is vacuum-saturated with water containing a dopant. Porosity is obtained by using Equation 1 (based on the equation proposed by Withjack [5].

$$\phi = \frac{CT_{wet} - CT_{dry}}{CT_{water} - CT_{air}} \qquad (1)$$

where,

CT_{wet} = Mean CTN for core fully saturated with water
CT_{dry} = Mean CTN of the dry core
CT_{water} = Mean CTN of the doped water
CT_{air} = Mean CTN of the air

Note that CT_{water} and CT_{air} are calculated from the scans of the sample bottles of the same size within the coreholder. There is also another technique for measuring porosity using CT, which is called the standards-based technique, which is discussed in detail in an associated publication [15]. Basically, in the standards-based technique porosity is calculated from the linear relationship between the CTN for air and the CTN for a representative calibration standard, and this technique also gives fairly accurate values.

Fig. 6 shows the slice-by-slice porosity distribution for a three-plug carbonate composite core from a Middle-Eastern reservoir[14]. The individual slices are as follows: Slices 1 through 7 represent Plug #26, Slices 9 through 15 represent Plug #157 and Slices 17 through 24 represent Plug #100, with slices 8 and 16 being the transition slices. The porosity values obtained from conventional core analysis (at 2,500 psi and room temperature) for the three plugs in the above sequence are 0.281, 0.234 and 0.243, respectively. CT-derived porosity values for the same plugs were 0.286, 0.240 and 0.248, respectively. Fig. 6 shows that regardless of whether the porosity is determined by the standards method or by the saturation method (equation 1), the average porosity values are very close. The differences seen in plug #100 may represent the difference between total and effective porosities in the heterogeneous core plug. saturation of water in this highly heterogeneous plug. It could also be simply due to insufficient saturation of the core plug following vacuum-saturation.

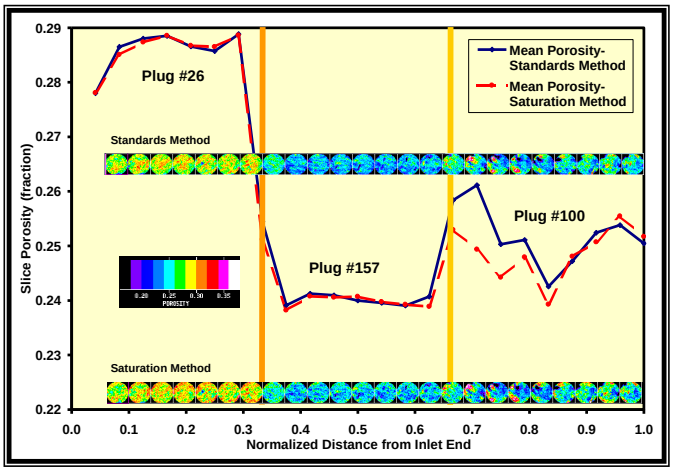

Fig. 6. CT-derived slice-by-slice porosity of a three-plug composite core showing difference between the standards-based and the saturation techniques [16].

CT-assisted coreflooding tests can be of two types: tests with as-is or wettability-preserved core plugs; and tests with cleaned, extracted and dried core plugs. The former is less common because it is prone to more uncertainties and errors in measurements because the core plugs have to be completely extracted, cleaned and dried after the test (the process may damage the plugs) and put back in the original order at the exact same location inside the coreholder. This would allow porosity, absolute permeability and saturation measurements but voxel-by-voxel image subtraction will be very difficult to do as minor positioning inaccuracy can lead to huge differences.

It should be noted that regardless of the test type, the use native fluids is almost not practiced in CT-assisted SCAL tests because of many practical limitations. The high brine salinity, sometimes exceeding 200,000 ppm, can have detrimental effects on the fluid lines and sensitive equipment, and the live oil can affect the sleeves and the flow lines and is difficult to remove from the experiment after the test. Usually, a synthetic brine with one or two orders of magnitude lower ppm and containing a dopant; and a refined or mineral oil, with properties compatible with reservoir oil, is used for two-phase flow experiments.

The following test sequence can be followed for a two-phase (oil-water) unsteady-state (JBN) CT-assisted coreflooding test with one or more wettability-preserved core plugs.

A. Mount the core plug(s) inside the Hassler sleeve inside the coreholder after marking the locations with an indelible marker, apply confining pressure and reservoir temperature. Continuously record the differential pressure during all flow sequences. During all scanning operations start from the same starting position on the CT table and make sure the coreholder does not move.
B. Inject 10 PV of doped brine (e.g., 5% NaI in water) to remove the movable oil. Scan at fixed intervals (or continuous for multislice CT).
C. Inject a total of 20 PV of doped brine to establish the initial **Sor**. At steady-state, measure the differential pressure to calculate effective permeability at the residual oil saturation, **Sor**.
D. Scan the core after injecting 0.2 PV of oil (to view the Buckley-Leverett shock front).
E. Scan the core after injecting 10 PV of oil.
F. Scan the core after injecting a total of 20 PV of oil, to establish the baseline for irreducible water saturation, **Swir**.
G. Scan the core after injecting 10 PV of brine.
H. Scan the core after injecting a total of 20 PV of brine to obtain the residual oil saturation, Sor baseline.
I. Take the core plug(s) out carefully after bringing temperature and pressure down; put the core(s) in a Soxhlet extractor (or similar extraction device) and use one or more solvents (toluene, methylene chloride, hexane, etc.) to remove all the fluids. Dry the sample in an oven. Measure core porosity (using helium porosimetry) and air permeability (to be used as a reference) before mounting the cores inside the Hassler sleeve and coreholder following the markings in step A.
J. Apply confining pressure and reservoir temperature and start pulling vacuum. Scan the core(s) from the same starting position as in step A.
K. Scan the core following saturation with the doped brine.
L. Scan the core again after circulating 5 PV of brine.

Typical CT-scan sequence for an unsteady-state (JBN) two-phase oil-water relative permeability test [16], in which the in-situ saturations are calculated using CT, is given below.

a. Scan the core when it is under vacuum.

b. Scan core immediately after saturating it with a brine (containing 5% NaI by weight in water).

c. Scan the core after circulating 5 PV of brine.

d. Scan the core after circulating 10 PV of brine to ensure full saturation and to establish the 100% water saturation baseline. At steady-state, measure the differential pressure to calculate the absolute permeability.

e. Start injecting single phase oil for the JBN method. Stop oil injection after injecting about 0.2 PV of oil. Quickly scan to view the Buckley-Leverett shock front.

f. Continue injecting oil. Scan the core after injecting 10 PV of oil.

g. Scan the core after injecting a total of 20 PV of oil to establish the baseline for irreducible water saturation, **Swir**.

h. Start injecting doped brine. Stop injecting after injecting about 0.2 PV of brine to quickly scan to view the Buckley-Leverett shock front (optional)

i. Continue injecting brine. Scan the core after injecting 10 PV of brine.

j. Scan the core after injecting a total of 20 PV of brine to obtain the residual oil saturation, **Sor**.

Fig. 7 shows the CT number profiles for four (i.e., sequences d, e, g and j) of the nine sequences described above, for an unsteady-state relative permeability experiment. The two extreme ones (100% water and 20 PV oil injected) generally follow the shapes of the underlying porosity distribution plots seen in Fig 6.

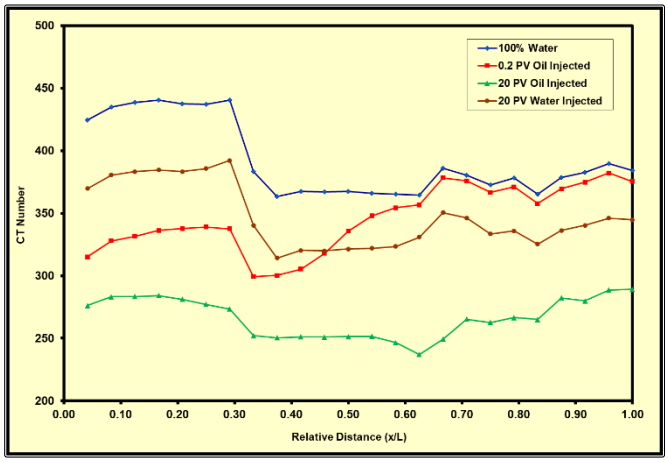

Fig. 7. CTN profiles during a coreflooding test using a three-plug composite core [16] (sequences d, e, g and j).

Fig. 8 shows the calculated in-situ water saturation profiles for the same four sequences described above. Sequence d (line with blue symbols) represents the 100% **Sw** and Sequence g (line with green symbols) represents the **Swir** of about 34% (or maximum **So** of about 66%), which is calculated independently from material balance. Both of these lines are based on the assumption that at each scan location water saturation and oil saturation have reached their highest respective values due to the injection of 10 PV of brine and 20 PV of oil, respectively. These maybe valid assumptions due to the relatively large volumes of fluids injected prior to reaching that state. Once, these two baselines have been established, it is possible to calculate saturation value at any point during any fluid sequence simply from the CT number for that sequence, as shown in Fig. 8 for the 0.2 PV of oil injected (sequence showing the Buckley-Leverett shock front) and also for the end of waterflooding (20 PV of water injected).

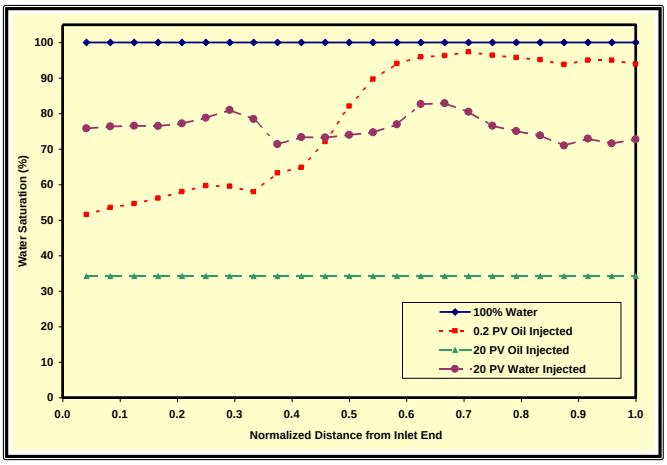

Fig. 8. CT-derived saturation profiles during coreflooding of the three-plug composite core [16] (sequences d, e, g and j).

It should be noted that for this relative permeability test [16], the liquid flow rate was 10 cm^3/min, which meets the Rapoport and Leas' [17] stabilized flow criterion. These tests also give an estimate of **Sor**, which is important for reserve estimates.

7 Image Processing

Although average attenuation data for slices from different scan sequences are sufficient to calculate in-situ saturations. the ability to perform a voxel-by-voxel subtraction opens many possibilities, including 3D animation of coreflooding. A good image processing software should be able to allow voxel-by-voxel image subtraction of a sequence of CT slices from another sequence of slices. In order to be successful, the coreholder should not move between individual flow sequences and the CT-scanner's positioning system should provide sufficient repeatability each time. Also, during the image processing, the circular region-of-interest (ROI) should have the same size for all the slices.

The simplest of image subtraction involves subtracting the matrix data from all the subsequent sequence images. Image subtraction allows the observation of minor flow anomalies, which helps our understanding of multiphase flow, especially in heterogeneous porous media. For a CT-supported two-phase (oil-water) relative permeability experiment [18], in which the water phase is doped, it is common to subtract the images of all subsequent sequences from the images corresponding to 100% water saturation. Fig. 9 shows an example of image subtraction for the same three-plug composite core for sequences 'd' through 'j' described above.

The snapshot for each sequence is taken from a 2D vertical cross-section of the composite core with injection taking place from the left. The Buckley-Leverett shock front during Sequence 'e' is quite evident, with invading oil on the left pushing the water in an almost piston-like displacement (some smearing may be due to viscous fingering or minor positional anomaly). The shock front has the same shape as the shock front seen in the corresponding saturation plot in Fig. 8. Image subtraction also allows good 3D visualization with animation of coreflooding sequences, which can be very useful. If the image processing software allows flexible color scales, individual phases within certain saturation range can be very easily identified using these new color scales.

8 Other Applications

A CT flow setup can be used for designing multiple applications involving flow in porous media. Fig. 10 shows an example of using **emulsified acid for wormhole creation** in a carbonate core. Emulsified acid is injected into a brine-saturated small carbonate core plug. Continuous end-to-end scans of the core during this test allowed the researchers to better understand the process of wormhole creation and the effect of retardation used for this set of experiments. In Fig. 10 the acid is injected from the left and it exits from the right after creating the wormhole, shown in brown. Image subtraction was used to observe the minor changes within the core plug. After a few trial-and-error cases involving oil-soluble and water-soluble dopants, a water-soluble dopant was used in the brine phase in order to obtain maximum contrast during acid injection, which was encapsulated in diesel [19].

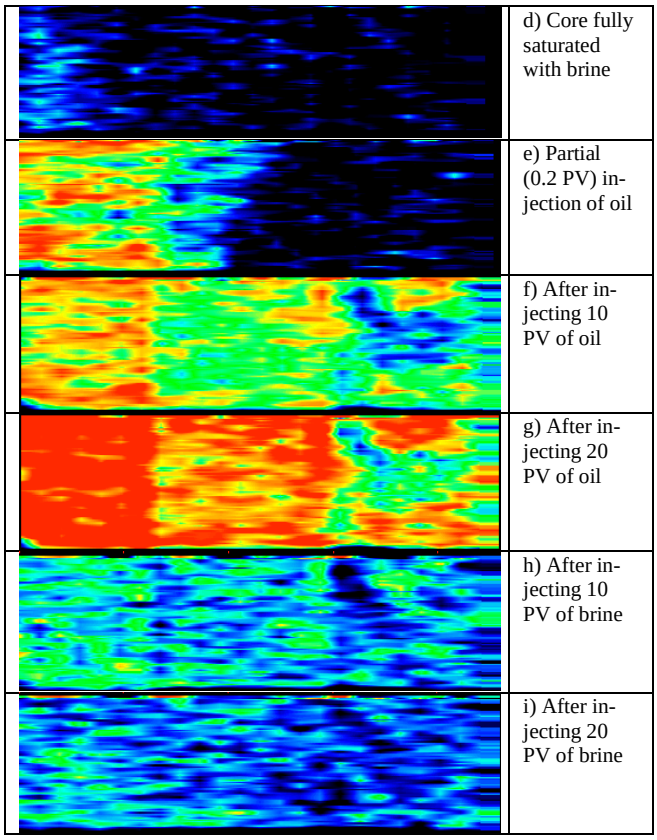

Fig. 9. Snapshots showing saturation changes in a 2-D vertical cross-section (sagittal slice) during a waterflooding test on a three-plug carbonate core [18].

CT flow visualization setup was also successfully used to calculate **pore volume compressibility** of core plugs in a non-destructive way. For this particular set of tests, a fully vacuum-saturated core plug was scanned at several locations first. Then it was compressed gradually by the confining fluid while leaving the outlet open and connected to a sensitive balance to accurately monitor the effluent coming out of the core at each confining pressure setting. The density changes at each slice location within a fixed ROI were then used for calculating the pore volume compressibility. The advantage of the CT-based technique is that instead of having one set of pore volume compressibility versus net pressure plot, one can obtain a band of such plots, showing the variability of such data. More details on this technique can be found in Ref. [20]. Fig. 11 is an example of pore volume compressibility (with varying confining pressure, C_{pc}) versus net confining pressure plot for a small core plug showing the results of the two half cycles of compression.

Although for three phase saturation measurement it is normal to use scans at two different energies at the same locations 13], sometimes single energy scans can be used to observe certain behavior of reservoir fluids during three-phase flow in porous media. This can be done by matching the CT numbers of two of the three fluid phases. The fluid matching process involves scanning multiple sample bottles with different

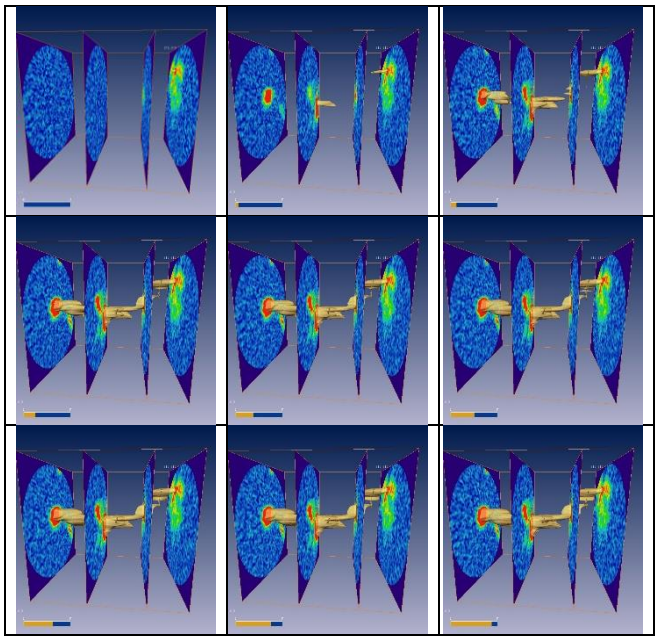

Fig. 10. Snapshots showing saturation changes based on 3-D data during an emulsified acid injection test on a carbonate core plug [19].

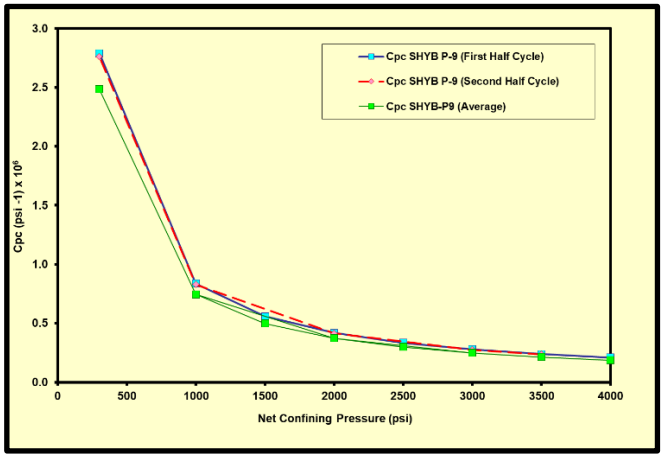

Fig. 11. Plot of pore volume compressibility with variable confining stress (C_{pc}) versus net confining pressure for a carbonate core plug, using a CT flow visualization setup [19].

concentrations of oil-soluble and water-soluble dopants in oil and water, respectively [21]. In order to avoid interphase mass transfer, all the fluids (water, benzyl alcohol, decane) were pre-mixed in a large bottle and separated prior to making the solutions using the dopants. Fig. 12 includes some interesting images observed during injection of NaI doped brine (representing the water phase) into a core saturated with benzyl alcohol doped with iodo-dodecane (representing the oil phase) and undoped decane. The injection is from the left. The horizontal slice shows viscous fingering of water (light blue and yellow) into the denser benzyl alcohol phase (dark blue), but interestingly the decane phase (yellow-red, on the right), whose CT number was matched with that of the water (yellow-green on the left), shows the decane moving like a piston ahead of the benzyl alcohol (blue) phase. The vertical slice from the same sequence of coreflooding shows gravity segregation, as the denser benzyl alcohol (blue) tries to settle to the bottom. These single-energy scan experiments were designed to physically observe the Buckley-Leverett shock front and match with the calculated saturation profiles. The lowermost image shows that the match on the average between the calculated and in-situ saturations is very good in spite of some apparent flow anomalies. Details of these experiments can be found in the literature [21].

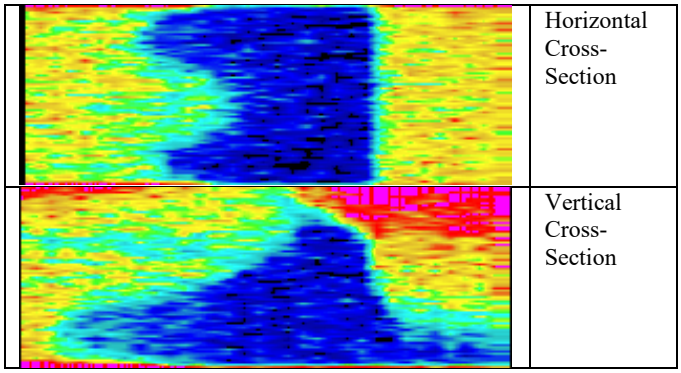

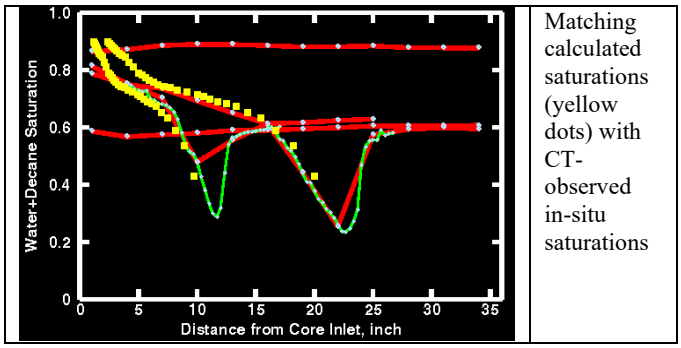

Fig. 12. Horizontal cross section showing viscous fingering of the water phase at the left and piston like displacement of the decane phase on right. Vertical cross-section showing gravity segregation of the denser benzyl alcohol phase. Red lines show observed saturations from coarse scans, green lines show saturations from fine scans and the yellow squares show calculated saturations using the three-phase extension of the Buckley-Leverett theory [21].

9 Summary

This paper discusses the use of CT-scanning for multiphase flow visualization and quantification, which has been used for over 37 years in the oil industry. Some guidelines have been provided for future researchers for equipment selection and setup, dopant selection and experiment design, with examples. The paper also discusses some successful applications of CT-scanning. With the introduction of the high-speed high-resolution micro-CT, new research pathways are expected to be created, which can help the petroleum engineers and geoscientists to understand the reservoir rocks better.

10 Acknowledgments

The author expresses his deep appreciation for his mentors Abraham Grader, Paul Hicks and Phillip Halleck for their help and support. The author also thanks his friends Otman Algadi and Abdulrahman AlQuraishi, and former colleagues at the Saudi Aramco, Sultan Al-Enezi, Aon Khamees, Jim Funk and Ahmad Harbi. The author appreciates the support of Bob Kehl of Kehlco, Inc. for his VoxelCalc petrophysical image processing software, which was used for generating some of the images.

Nomenclature

CTN	CT Number
CTwet	Mean CTN for core fully saturated with
CT_{dry}	Mean CTN of the dry core
CT_{water}	Mean CTN of the doped water
CT_{air}	Mean CTN of the air

Cpc	Pore volume compressibility with varying confining pressure
JBN	Johnson-Bossler-Naumann method for calculating relative permeability
NaI	Sodium Iodide (a dopant)
ppm	parts per million
Sw	Water saturation (fraction)
So	Oil saturation (fraction)
Swir	Irreducible water saturation (fraction)
Sor	Residual oil saturation (fraction)
ROI	Region of interest

References

1. S.Y. Wang, S. Ayral, C.C. Gryte, SPE Journal, Feb. (1984).
2. V. Cromwell, D.J. Kortum, D.J. Bradley, SPE Ann, Tech. Conf. Sep. (1984). doi: https://doi.org/10.2118/13098-MS.
3. H.J. Vinegar, S.L. Wellington, Rev. of Sc. Instr. **58**, Jan. (1987).
4. S.L. Wellington, H.J. Vinegar, J Pet Tech. **39** (1987). doi: https://doi.org/10.2118/16983-PA.
5. E.M. Withjack, SPE Form. Eval. **3** (1988). doi: https://doi.org/10.2118/16951-PA
6. E.J. Peters, W.D. Hardham, J. Pet. Sc. and Eng. **4**, 2, May (1990). doi: https://doi.org/10.1016/0920-4105(90)90023-V.
7. A. Kantzas, In Situ, **14**, 1, (1990).
8. S. Akin, A.R. Kovscek, Annual Report of SUPRI TR 127, Stanford University, Stanford, CA, Aug. (2001).
9. E.M. Withjack, C. Devier, G. Michael, Pres. at the SPE Western Regional/AAPG Pacific Section Joint Meeting, Long Beach, California, May (2003). doi: https://doi.org/10.2118/83467-MS.
10. P. Zhang, Y.I. Lee, J. Zhang, Micron, **124**, Sep. (2019), https://doi.org/10.1016/j.micron.2019.102702.
11. S. Siddiqui, J. Sun, J., M.J. Burgess, M.S. Al-Buraiki, Jour. Nature Science and Sust. Tech. (JNSST), **4**, 4, 2011.
12. O.A. Algadi, MS Thesis in Petroleum Engineering, Texas Tech University, Lubbock, Texas, May 2012.
13. A. Sahni, J. Burger, M. Blunt, Pres. at the SPE/DOE Improved Oil Recovery Symp., Tulsa, Oklahoma, Apr. (1998). doi: https://doi.org/10.2118/39655-MS.
14. A.A. AlQuraishi, S. Siddiqui, S, O.A. Algadi, Pres. at the 13th Offshore Mediterranean Conference and Exhibition in Ravenna, Italy, Mar. (2017).
15. S. Siddiqui, E3S Web Conf. **367**, Art. No. 01013 (2023). doi: https://doi.org/10.1051/e3sconf/202336701013
16. S. Siddiqui, J.J. Funk, A.A. Khamees, Pres. at the 2000 SCA Symp., Abu Dhabi, UAE, Oct. (2000). SCA pap. no. 2000-06.
17. L.A. Rapoport; W.J. Leas, J Pet Technol 3 (03), 83–98. Doi: https://doi.org/10.2118/951083-G.
18. S. Siddiqui, S. and A. Khamees, SPE-106334-MS, pres. at the 2005 SPE Technical Symposium of Saudi Arabia Section, Dhahran, Saudi Arabia. https://doi.org/10.2118/106334-MS.
19. S. Siddiqui, H.A. Nasr-El-Din, A.A. Khamees, Jour. Pet. Sc. and Eng, **54**, 3-4, Dec. (2006). doi: https://doi.org/10.1016/j.petrol.2006.08.005.
20. S. Siddiqui, J.J. Funk, A.M. Al-Tahini, SPE Res. Eval. & Eng., **13**, 1. Feb. (2010). doi: https://doi.org/10.2118/116313-PA.
21. S. Siddiqui, P.J. Hicks, A.S. Grader, Jour. Pet. Sc. and Eng, **15**, 1, Jul. (1996). doi: https://doi.org/10.1016/0920-4105(95)00056-9.